Materials International
Open Access Journal (ISSN: 2668-5728)

*Review*
**Volume 6, Issue 3, 2024, 28**
https://doi.org/10.33263/Materials63.028

# Convective Diffusive Mass Transfer over a Rectangular Channel in the Human Cardio System

**Punith Kumar [1], Sravan Kumar Thavada [2,*], Vijaya KumarAvula Golla [3]**

1. Department of Mathematics, Aditya College of Engineering and Technology, Bangalore-64,KA, India; drpunithkumardn@outlook.com(P.K.D.N);
2. Department of Mathematics, Atria Institute of Technology, Bangalore-24,KA, India; thavadasravankumar@gmail.com (S.K.T);
3. Department of Mathematics, SAS, Vellore Institute of Technology, Vellore; vijayakumarag@vit.ac.in (V.K.A.G);

* Correspondence: thavadasravankumar@gmail.com;

Scopus Author ID 56872884700
**Received: 26.05.2023; Accepted: 6.01.2024; Published: 10.09.2024**

**Abstract:** In the present analysis, a study on convective-diffusive mass transfer of injected drug in a couple of stress fluid flows through a rectangular channel, with the effects of suction and injection, is considered. An attempt is made to study the effect of suction and injection on convective diffusive mass transfer in a flow of couple stress fluid. The governing equations in the above situation are solved analytically and depicted graphically. The computational results obtained are found to be in good agreement with the physical model for various parameters of the physical configuration.

**Keywords:** couple stress fluid; convective-diffusive mass transfer; suction and injection.



## 1. Introduction

In the current era of computational modeling, the needs of government, industry, and other interdisciplinary branches invoke hardcore research and developments in the field of fluid dynamics. Due to its application in multiple disciplines, new problems are taking birth to create scope for analyzing fluid flow behavior in various sectors. Theoreticians are developing simulations for larger fluids systems to understand and explore more and solve the problems that arise, providing accurate solutions. However, there is still a need for more advanced methods to crack complex problems. Theoretical and computational fluid dynamics provides a forum for scientists, mathematicians, and engineers to address the issues and challenges emerging in fields concerning fluid flow aspects. Regarding innovation in fluid flow theory, understanding fluid flow behavior under various cases still leads to the front row of analysis. The present study analyzes the couple stress fluid flow to measure the mass transfer rate through the convection and diffusion processes.

Couple stress is a force that acts on fluid to induce rotation on the fluid in local form. The internal stress in such fluids is the result of different structures in fluids. This stress can affect the flow behavior and other fluid properties. The couple stress theory has wide applications in biomechanics like biofluids, pumping fluids, and liquid crystals. Srivastava [1] presented a couple of stress fluid models by considering blood flow to analyze mild stenosis effects. Devakar *et al*. [2] solved Stoke’s problem for couple stress fluid using Laplace transform method. Velocity profiles are studied for different couples stress Reynold’s number. Devakar *et al*. [3] presented the Couette flow of a couple of stress fluids between parallel plates and obtained an exact solution for the problem. Ramzan *et al*. [4] presented a three-dimensional analysis of Newtonian heating effects on stretching surfaces. Numerical solutions describing skin friction and Nusselt number for different parameters are tabulated. Sravan Kumar [5] studied two-dimensional reducing PDEs to coupled nonlinear ODEs. The numerical solution is obtained using the shooting technique coupling with the RK method. Pei-Ying Xiong *et al*. [6] examined Poiseuille flow considering a couple of stress fluids flowing between parallel plates. They investigated thermal conductivity, radiation, and other effects. The governing equations are solved numerically, and the results are depicted graphically.

Shilpa *et al*. [7] discussed the Soret and Dufour effects to analyze convective diffusive mass transfer of couple stress fluid flow in a vertical channel with external magnetic field application. The governing nonlinear equations are solved using the Galerkin method, and results are depicted using Artificial Neural Networks. Sravan Nayeka *et al*. [8] presented the Landau model to study the effect of gravity modulation of couple stress fluid through porous media. The results are obtained using Mathematica software. Prasad *et al*. [9] presented a non-Newtonian model by considering a couple of stress fluids with nanoparticles. The governing equations are solved using the Keller-Box method. Mkhatshwa *et al*. [10] presented a multi-domain bivariate spectral relaxation method to study MHD flow of couple stress fluid over a stretching sheet in oscillating form with soret and other related effects. Raghunath *et al*. [11] studied stability analysis of couple stress fluid through a porous medium. A numerical analysis is performed on the sucrose system. Muhammad *et al*. [12] analyzed Carreau fluid flow by considering couple stress and Marangoni convection. The phenomenon is modeled using the Homotopy analysis method, and the results are depicted graphically. Ramesh [13] explored the effects of Hall currents, convection, and slip boundary conditions on nanofluids through porous microchannels. The resultant system is solved using the RK method, and graphs indicate various fluid flow quantities.

One of the essential modes of heat transport is convection. Convection occurs by diffusion and advection. The most common form of transport, yet complex, is convective mass transfer. Mass transfer is the last mechanism in transport phenomena, and it occurs through the analysis of diffusion and mass convection. The mathematical equation that describes the mass transfer is the convective diffusion equation. Applications of convection-diffusion equations include modeling of heat transfer in fluids, mass transfer in porous media, and chemical reactions. Sankarasubramanian and Gill [11] presented a dispersion model explaining interphase transport using the first principle concept. Because of the complexity of the problem, evaluation is done for a time only, which is asymptotic. Vafai and Tien [12] discussed mass transfer through convection and diffusion in the case of porous media. They explained how mass flux makes significant changes in porosity. Zhang *et al*. [13] presented experimental work on convective mass transfer through porous media. They emphasized mass transfer near the impermeable boundary.

Nandeppanavar *et al*. [14] explained the significance of lower critical solution temperature to improve cooling effects during convection and diffusion. The case was studied using microchannels, and the results depict that a suitable temperature range improves cooling performance. Ashis Kumar Roy *et al*. [15] developed a two-fluid model presenting a simulation of Eringen micropolar fluid. The closed-form solutions are obtained using the Gill decomposition method. Zhang *et al*. [16] investigated the effects of thermal diffusion during heat and mass transfer considering a third-grade fluid. The resulting coupled partial differential equations are reduced to ordinary differential equations and solved using the BVP4C method.

Nandeppanavar *et al*. [17] presented the analysis of a double-diffusive mixed convective stream over a vertical plate. They investigated the Biot number and graphically depicted the effect of various flow parameters. Ashis Kumar Roy *et al*. [18] presented a robust model examining the transport species equation to analyze carrier fluid flow in stenosed arterial geometry. The resulting boundary value problems are solved, and multiple-scale solutions are obtained. Sushma *et al*. [19] presented the analysis of DES performance in the human body using numerical techniques. They reviewed numerous models explaining the mathematical methods to control parameters. Weijermars [20] studied a probability solution for molecular diffusion in porous media. The computation for the problem is performed by implementing the Gaussian pressure method. Abbas *et al*. [21] investigated thermal diffusion effects on third-grade fluid. The nonlinear PDE is solved using bvp4c methods, and MATLAB results are computed. Zhao and Yang [22] studied the effects of coupled diffusion and magnetic effect on convective fluid flow. The associated parameters Nusselt and Sherwood numbers are evaluated using graphs.

In boundary layer theory, suction is one of the premium methods to control the boundary layer. This reduces the body drag in an external flow, reducing channel energy loss. The suction process becomes more effective in the case of the porous medium. Suction decreases the thickness of the boundary layer to be more effective in the stability analysis of layers on the boundary.

In fluid mechanics, injection is introducing a fluid into another fluid. Its application is in hydraulic fracturing, boundary layer control, and drag reduction. During the injection process, understanding the volumetric distribution of injected fluid is necessary for many engineering processes. In recent days, convective boundary layer and heat transfer have gained major concentration in industry and engineering activities. The applications of convective flow are to handle hot wire, petroleum storage, filter process, and nuclear waste disposal. Obulesu *et al*. [23] worked on a theoretical analysis of Marangoni convection flow in carbon nanotubes with porous surfaces. For the analysis, the suction and injection process is considered. Suitable transformations solve the resulting differential equations. Bagh Uddin *et al*. [24] explored the significance of suction /injection for mixed convection in micropolar fluid flow. The resulting PDE is solved using finite element analysis. Islam *et al*. [25] investigated heat and mass transfer over the nonuniform porous plate. The transport flow regime governed by PDE is solved, and results are presented graphically. Bagh *et al*. [26] analyzed incompressible micropolar nanofluids flow with suction/injection application. The governing equations are solved numerically using the RKF-45 method. Anil Kumar *et al*. [27] presented an article on Short and Dufour's impact on natural convective flow through porous media with the suction/injection process.

Though many forms of research are happening, there is still scope to identify the niche areas to develop and implement mathematical models to obtain solutions for various complex, unsolved cases. This paper attempts to solve one such case, and a model is presented to address the issue.

## 2. Mathematical Description

Let us consider the plane Poiseuille flow of stokes couple stress fluid flowing through a channel of height $h$ as shown in Figure 1.

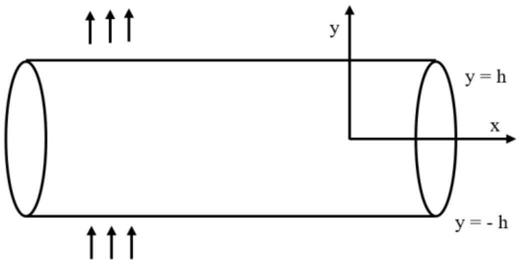


**Figure 1.** Physical configuration.

The governing equations for such a flow are

$$v\frac{\partial u}{\partial y}=-\frac{\partial p}{\partial x}+\left(\mu\frac{\partial^2 u}{\partial y^2}-\eta\frac{\partial^4 u}{\partial y^4}\right) \quad (1)$$

Subject to boundary conditions

$$u=u_0P \quad \text{at} \quad y=h \quad (2a)$$

$$u=-u_0P \quad \text{at} \quad y=-h \quad (2b)$$

$$\frac{d^2u}{dy^2}=0 \quad \text{at} \quad y=\pm h \quad (2c)$$

Introducing the following non-dimensional quantities

$y^*=\dfrac{y}{h}\ u^*=\dfrac{u}{u0}$, equations (2) to (2c) reduce to the following form

$$\frac{d^4u}{dy^4}-a\frac{d^2u}{dy^2}+b\frac{du}{dy}=P \quad (3)$$

$$u=0,\quad \frac{d^2u}{dy^2}=0 \quad at \quad y=\pm 1 \quad (4)$$

Where $a=\dfrac{\mu h^2}{\eta},\quad b=a\,\mathrm{Re},\ \mathrm{Re}=\dfrac{\mu_0 h}{\mu}, P=-\dfrac{h^4}{\eta\mu_0}\dfrac{\partial p}{\partial x}$ and $v$ = coefficient of Kinematic viscosity, $R_e$ = Reynolds number, $u$ = dimensionless velocity component of the flow, $\dfrac{\partial p}{\partial x}$ = constant pressure gradient.

Solving (2) using (3), we get the velocity profile as

$$u(y)=-\frac{p}{b}\left[\alpha_4+\alpha_3e^{\gamma y}+\alpha_2e^{\alpha y}\cos\beta y+\alpha_1e^{\alpha y}\sin\beta y-y\right] \quad (5)$$

The average velocity is given by

$$\bar{u}=\frac{1}{2}\int_{-1}^{1}udy=-\frac{2P}{b}\left[\alpha_4+\frac{\alpha_3}{\gamma}\sin\mathrm{h}\,\gamma+\frac{1}{\alpha^2+\beta^2}\left\{\cosh\alpha\sin\beta\left(\alpha\alpha_1+\beta\alpha_2\right)+\sinh\alpha\cos\beta\left(\beta\alpha_1+\alpha\alpha_2\right)\right\}\right] \quad (6)$$

## 3. Dispersion Model

Let $c$ be the concentration distribution in the fluid. Then we introduce $c(0,x,y)$ which is the initial slug input into the flow and $c(t,x,y)$ is the local concentration of the solute. The concentration $c$ satisfies the convective-diffusion equation

$$\frac{\partial c}{\partial t}+u(y,t)\frac{\partial c}{\partial x}=D\left(\frac{\partial^2 c}{\partial x^2}+\frac{\partial^2 c}{\partial y^2}\right) \quad (7)$$

With boundary conditions

$$c(0,x,y)=c_0\,\psi_1(x)Y_1(y) \tag{8a}$$

$$-D\frac{\partial c}{\partial y}=k_s c \text{ at } y=h \tag{8b}$$

$$-D\frac{\partial c}{\partial y}=k_s c \quad at \quad y=-h \tag{8c}$$

$$C(t,\infty,y)=\frac{\partial c}{\partial x}(t,\infty,y)=0 \tag{8d}$$

Where $c_0$ is the reference concentration, $k_s$ is the reaction rate constant, $D$ is the diffusion coefficient.

In non-dimensional form, (7) to (8d) can be rewritten as

$$\frac{\partial\theta}{\partial r}+U\frac{\partial\theta}{\partial X}=\frac{1}{P_e^2}\frac{\partial^2 c}{\partial X^2}+\frac{\partial^2\theta}{\partial\xi^2} \tag{9a}$$

$$\theta(0,X,\xi)=\psi(X)Y(\xi) \tag{9b}$$

$$\frac{\partial\theta}{\partial\xi}=-\beta\theta \quad at \quad \xi=+1 \tag{9c}$$

$$\frac{\partial\theta}{\partial\xi}=-\beta\theta \quad at \quad \xi=+1 \tag{9d}$$

$$\theta(\tau,\infty,\xi)=\frac{\partial\theta}{\partial x}(\tau,\infty,\xi)=0 \tag{9e}$$

Where $\xi=\dfrac{y}{h},\tau=\dfrac{Dt}{h^2},\theta=\dfrac{c}{c_0},X=\dfrac{Dx}{h^2\bar{u}},\ U=\dfrac{u}{\bar{u}},\ P_e=\dfrac{h\bar{u}}{D},\ \beta=\dfrac{k_s h}{D}$.

Using the generalized dispersion model proposed by Sankara Subramanian and Gill [11], the solution of (9a) using (9b) to (9e), we get

$$\theta=\sum_{k=0}^{\infty} f_k(\tau,\xi)\frac{\partial^k\theta_m}{\partial X^k} \tag{10}$$

where $\theta_m=\int_{-1}^{1}\theta\,d\xi$ is the dimensionless mean concentration (11)

Integrating (9a) w.r.t $\xi$ between -1 and 1 we get

$$\frac{\partial\theta_m}{\partial r}=\frac{1}{P_e^2}\frac{\partial^2\theta_m}{\partial X^2}+\frac{1}{2}\left|\frac{\partial\theta_m}{\partial\xi}\right|_{-1}^{1}-\frac{1}{2}\frac{\partial}{\partial X}\int_{-1}^{1}U\theta\,d\xi \tag{12}$$

Let us introduce the dispersion coefficient

$$\frac{\partial\theta_m}{\partial r}=\sum_{i=0}^{\infty}K_i(\tau)\frac{\partial^i\theta_m}{\partial X^i} \tag{13}$$

The process of distributing $\theta$ is diffusive in nature.

The values $K_i(\tau)$ can be obtained from the following relation:

$$K_i(\tau)=\frac{\delta_{i,2}}{Pe^2}+2\frac{\partial f_i}{\partial\xi}(\tau,1)-\frac{1}{2}\int_{-1}^{1}f_{i-1}Ud\xi \quad i=0,1,2..... \tag{14}$$

Where $f_{-1}=f_{-2}=0,\delta_{i,2}$ is the Kronecker delta defined by $\delta_{ij}=\begin{cases}1, & for\ i=j\\ 0, & for\ i\#j\end{cases}$

The existence of $\frac{\partial f_i}{\partial \xi}$ in (14) affects the higher order $K_i$ values due to non-zero solute flux $K_0(\tau)$. Since $K_3(\tau)K_4(\tau),.....$ they are negligibly small compared to $K_0(\tau), K_1(\tau), K_2(\tau)$ those that are dominant, we truncate the equation (14) after the term $K_2(\tau)$ without causing series errors.

Equation (14) reduces to the following form due to truncation

$$\frac{\partial \theta_m}{\partial \tau} = K_0(\tau)\theta_m + K_1(\tau)\frac{\partial \theta_m}{\partial X} + K_2(\tau)\frac{\partial^2 \theta_m}{\partial X^2} \tag{15}$$

To solve (15), we need the following values $K_i(\tau)$, $for\, i = 0,1,2\, and\, f_k$ $for\, k = 1,2,3......$. Hence, using (10) into (8 a) and (11) to get the set of partial differential equations given below:

$$\frac{\partial f_k}{\partial \tau} = \frac{\partial^2 f_k}{\partial \xi^2} - Uf_{k-1} + \frac{1}{Pe^2} f_{k-2} + \sum_{i=0}^{k} f_{n-i}K_i \quad k = 0,1,2,... \tag{16}$$

Equation (10) can be solved using the boundary conditions. To find $\theta_m\, and\, f_k$ the required initial and boundary conditions are

$$\theta_m(0, X) = \frac{1}{2}\int_{-1}^{1} \theta\, d\xi \tag{17a}$$

$$f_k(0,\xi) = 0\, and\, f_k(\tau,0) = finite\ for\ \ k = 1,2,3,....... \tag{17b}$$

$$\frac{\partial f_k}{\partial r}(\tau,1) = -\beta f_k(\tau,1) \tag{17c}$$

$$\theta_m(\tau,\infty) = \frac{\partial \theta_m}{\partial X}(\tau,\infty) = 0 \tag{17d}$$

We have $\frac{1}{2}\int_{-1}^{1} f_k\, d\xi = 0$ (by the definition of $\theta_m$) (18)

The functions $f_0$ and exchange coefficient $K_0$ are obtained from the following:

$$K_0(\tau) = \frac{1}{2}\left|\frac{\partial f_0}{\partial \xi}\right|_{-1}^{1} \tag{19}$$

And $\frac{\partial f_0}{\partial \tau} = \frac{\partial^2 f_0}{\partial \xi^2} - K_0 f_0$ (20)

The boundary conditions to solve (20) are (17a) to (17d).

The solution of (20) may be formulated as

$$f_0(\tau,\xi) = e^{-\int_0^{\tau} K_0(\tau)d\tau} g_0(\tau,\xi) \tag{21}$$

Where $g_0(\tau,\xi)$ must satisfy $\frac{\partial g_0}{\partial \tau} = \frac{\partial^2 g_0}{\partial \xi^2}$ (22a)

With boundary conditions

$$g_0(0,\xi) = f_0(0,\xi) = \frac{Y(\xi)}{\frac{1}{2}\int_{-1}^{1} Y(\xi)\, d\xi} \tag{22b}$$

$$\frac{\partial g_0}{\partial \xi}(\tau,1)=-\beta g_0(\tau,1),\ g_0(\tau,1)=finite \tag{22c}$$

The solution of (22a) using (22b) and (22c) is

$$g_0(\tau,\xi)=\sum_{n=0}^{\infty}A_n e^{-\mu_n^2\tau}\cos\mu_n\xi \tag{23a}$$

Where $A_n=\dfrac{2\int_{-1}^{1}Y(\xi)\cos\mu_n\xi d\xi}{\left[1+\dfrac{\sin 2\mu_n h}{2\mu_n}\right]\int_{-1}^{1}Y(\xi)d\xi}$ (23b)

And $\mu_n^{'}$ sare eigen values satisfying the following equation:

$$\mu_n\sin\mu_n=\beta\cos\mu_n\ for\ n=0,1,2,\ldots \tag{23c}$$

Using (21) in (20), we get

$$f_0(\tau,\xi)=\frac{\sum_{n=0}^{\infty}A_n e^{-\mu_n^2\tau}\cos\mu_n\xi}{\sum_{n=0}^{\infty}\frac{A_n}{\mu_n}e^{-\mu_n^2\tau}\sin\mu_n\xi} \tag{24}$$

Therefore,

$$K_0(\tau)=\frac{\sum_{n=0}^{\infty}(A_n\mu_n)e^{-\mu_n^2\tau}\sin\mu_n\xi}{\sum_{n=0}^{\infty}\frac{A_n}{\mu_n}e^{-\mu_n^2\tau}\sin\mu_n\xi} \tag{25}$$

As $\tau\to\infty$ the asymptotic representations for $f_0$ and $K_0$ are given by

$$f_0(\infty,\xi)=\frac{\mu_0}{\sin\mu_0} \tag{26}$$

$$K_0(\infty)=-\mu_0^2, \tag{27}$$

where $\mu_0$ is the first (lowest in magnitude) root of the equation

To find the asymptotic values $K_i,\ i=0,1,2,,$ we inject the solute into the flow. Then, for large values of time after injection, the steady state function $f_K(\xi)$ satisfy

$$\frac{d^2 f_K}{d\xi^2}+\mu_0^2 f_K=\frac{\bar{u}}{u}f_{K-1}-\frac{1}{P_e^2}f_{K-2}+\sum_{i=1}^{k}K_i f_{K-i}\ for\ k=1,2,3,\ldots \tag{28a}$$

With boundary conditions

$$f_k(0)=finite,\frac{\partial f_k}{\partial\xi}(1)=-\beta f_k(1),\ for\ k=1,2,3,\ldots \tag{28b}$$

$$\int_{-1}^{1}f_k d\xi=0,\ for\ k=1,2,3,\ldots \tag{28c}$$

Following the analysis explained in problem 4, we write

$$K_k=\frac{1}{\int_0^h f_0\cos\mu_0\xi d\xi}\int_0^h\left[\frac{\bar{u}}{u}f_{k-1}+\frac{1}{P_e^2}f_{k-2}-\sum_{i=1}^{k}K_i f_{k-i}\right]\cos\mu_0\xi d\xi \tag{29}$$

$$f_k=\sum_{j=0}^{\infty}B_{j,k}\cos\mu_j\xi\ for\ k=1,2,3,\ldots \tag{30}$$

Where $B_{j,k}=\dfrac{1}{\mu_j^2-\mu_0^2}\left[\dfrac{1}{P_e^2}B_{j,k-1}-\sum_{j=1}^{\infty}B_{j,k-1}-\left[1+\dfrac{\sin 2\mu_j h}{2\mu_j}\right]^{-1}\sum_{i=0}^{\infty}B_{i,k-i}I(j,l)\right]$ (31)

For $j \neq l$,

$$I(j,l)=\int_{-1}^{1}\frac{u}{\bar{u}}\cos\mu_j\xi\cos\mu_l\xi\,d\xi$$

$$=-\frac{P}{b\bar{u}}\left\{\begin{aligned}
&\alpha_4\left[\frac{\sin(\mu_j+\mu_l)}{\mu_j+\mu_l}+\frac{\sin(\mu_j-\mu_l)}{\mu_j-\mu_l}\right]+\\
&\frac{\alpha_3}{Y^2+(\mu_j+\mu_l)^2}\left[\gamma\sinh\gamma\cos(\mu_j+\mu_l)+(\mu_j+\mu_l)\cosh\gamma\sin(\mu_j+\mu_l)\right]+\\
&\frac{\alpha_3}{\gamma^2+(\mu_j-\mu_l)^2}\left[\gamma\sinh\gamma\cos(\mu_j-\mu_l)+(\mu_j-\mu_l)\cosh\gamma\sin(\mu_j-\mu_l)\right]+\\
&\frac{1}{\alpha^2+(\beta+\mu_j+\mu_l)^2}\left[\frac{1}{2}\sinh\alpha\cos(\beta+\mu_j+\mu_l)(\alpha\alpha_2+(\beta+\mu_j+\mu_l)\alpha_1)+\frac{1}{2}\cosh\alpha\sin(\beta+\mu_j+\mu_l)(\alpha\alpha_2+(\beta+\mu_j+\mu_l)\alpha_1)\right]+\\
&\frac{1}{\alpha^2+(\beta-\mu_j-\mu_l)^2}\left[\frac{1}{2}\sinh\alpha\cos(\beta-\mu_j-\mu_l)(\alpha\alpha_2+(\beta-\mu_j-\mu_l)\alpha_1)+\frac{1}{2}\cosh\alpha\sin(\beta-\mu_j-\mu_l)(\alpha\alpha_2+(\beta-\mu_j-\mu_l)\alpha_1)\right]+\\
&\frac{1}{\alpha^2+(\beta+\mu_j-\mu_l)^2}\left[\frac{1}{2}\sinh\alpha\cos(\beta+\mu_j-\mu_l)(\alpha\alpha_2+(\beta+\mu_j-\mu_l)\alpha_1)+\frac{1}{2}\cosh\alpha\sin(\beta+\mu_j-\mu_l)(\alpha\alpha_2+(\beta+\mu_j-\mu_l)\alpha_1)\right]+\\
&\frac{1}{\alpha^2+(\beta-\mu_j+\mu_l)^2}\left[\frac{1}{2}\sinh\alpha\cos(\beta-\mu_j+\mu_l)(\alpha\alpha_2+(\beta-\mu_j+\mu_l)\alpha_1)+\frac{1}{2}\cosh\alpha\sin(\beta-\mu_j+\mu_l)(\alpha\alpha_2+(\beta-\mu_j+\mu_l)\alpha_1)\right]
\end{aligned}\right\} \quad (32)$$

$For\ j=l$

$$I(j,l)=\int_{-1}^{1}\frac{u}{\bar{u}}\cos\mu_j\xi\cos\mu_j\xi\,d\xi$$

$$=-\frac{P}{2b\bar{u}}\left\{\begin{aligned}
&2\alpha_4+\frac{2\alpha_3}{\gamma}\sinh\gamma+\frac{2\alpha_2}{\alpha^2+\beta^2}[\alpha\sinh\alpha\cos\beta+\beta\cosh\alpha\sin\beta]+\\
&\frac{2\alpha_1}{\alpha^2+\beta^2}[\beta\sinh\alpha\cos\beta+\alpha\cosh\alpha\sin\beta]+\frac{\alpha_4}{\mu_j}\sin 2\mu_j+\\
&\frac{2\alpha_3}{\gamma^2+(4\mu_j)^2}\left[\gamma\sinh\gamma\cos 2\mu_j+2\mu_j\cosh\gamma\sin\mu_j\right]+\\
&\frac{\alpha_2}{\alpha^2+(\beta+2\mu_j)^2}\left[\alpha\sinh\alpha\cos(\beta+2\mu_j)+(\beta+2\mu_j)\cosh\alpha\sin(\beta+2\mu_j)\right]+\\
&\frac{\alpha_2}{\alpha^2+(\beta-2\mu_j)^2}\left[\alpha\cosh\alpha\sin(\beta-2\mu_j)+(\beta-2\mu_j)\sinh\alpha\cos(\beta-2\mu_j)\right]+\\
&\frac{\alpha_1}{\alpha^2+(\beta+2\mu_j)^2}\left[\alpha\cosh\alpha\sin(\beta+2\mu_j)+(\beta+2\mu_j)\sinh\alpha\cos(\beta+2\mu_j)\right]+\\
&\frac{\alpha_1}{\alpha^2+(\beta-2\mu_j)^2}\left[\alpha\cosh\alpha\sin(\beta-2\mu_j)+(\beta-2\mu_j)\sinh\alpha\cos(\beta-2\mu_j)\right]+\\
&\frac{2}{\alpha^2+\beta^2}\left[\cosh\alpha\sin\beta(\alpha\alpha_1+\alpha_1\beta)+\sinh\alpha\cos\beta(\alpha\alpha_2+\alpha_1\beta)\right]+\\
&\frac{1}{\alpha^2+(\beta+2\mu_j)^2}\left[\sinh\alpha\cos(\beta+2\mu_j)(\alpha\alpha_1+\alpha_1(\beta+2\mu_j))+\cosh\alpha\sin(\beta+2\mu_j)(\alpha\alpha_2+\alpha_2(\beta+2\mu_j))\right]+\\
&\frac{1}{\alpha^2+(\beta-2\mu_j)^2}\left[\sinh\alpha\cos(\beta-2\mu_j)(\alpha\alpha_1+\alpha_1(\beta-2\mu_j))+\cosh\alpha\sin(\beta-2\mu_j)(\alpha\alpha_2+\alpha_2(\beta-2\mu_j))\right]
\end{aligned}\right\} \quad (33)$$

We also obtain $K_1(\tau)\,and\,K_2(\tau)$ as

$$K_1(\tau)=\frac{I(0,0)}{\left[1+\dfrac{\sin 2\mu_0}{2\mu}\right]} \quad (34)$$

$$K_2(\tau)=\frac{1}{P_e^2}-\frac{\sin\mu_0}{\mu_0\left[1+\dfrac{\sin 2\mu_0}{2\mu_0}\right]}\sum_{j=0}^{\infty}B_{j,1}I(j,0) \quad (35)$$

The solution is obtained in one-half of the channel and $A_n$ can be rewritten due to symmetry as $\phi(\xi)\, given\, by\, \phi(\xi)=\begin{cases}1,\ 0\le\xi\le\xi_s\\ 0,\xi_s\le\xi\le 1\end{cases}$ (36)

The solution of (13) using (36) is

$$\theta_m=\frac{1}{2P_e\sqrt{\pi K_2(\infty)\tau}}\exp\left[K_2(\infty)\tau-\frac{\{K_1(\infty)\tau+X\}^2}{4(K_2(\infty)\tau)}\right] \tag{37}$$

## 3. Results and Discussions

Many physiological situations can be represented by a channel with a permeable wall, which results from suction and fluid injection, which affects the fluid flow and, hence, solute transfer. Hence, an exact analysis of solute transfer in a couple of stress fluids with the effects of suction and injection is carried out in Figure 2.

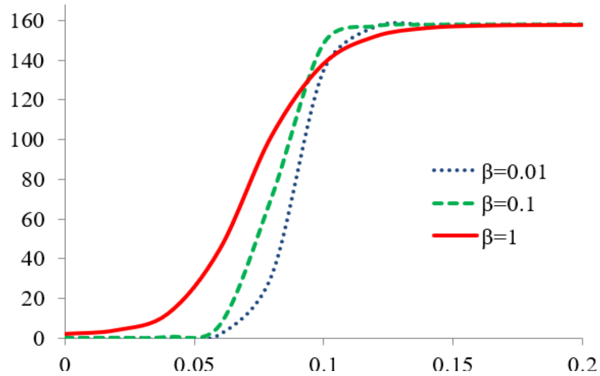


**Figure 2.** $K_0(\tau)$ versus $\tau$ .

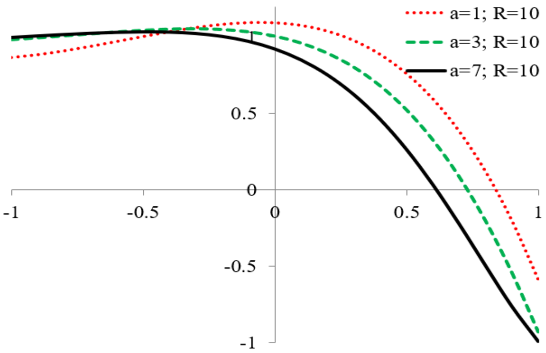


**Figure 3.** Velocity profile.

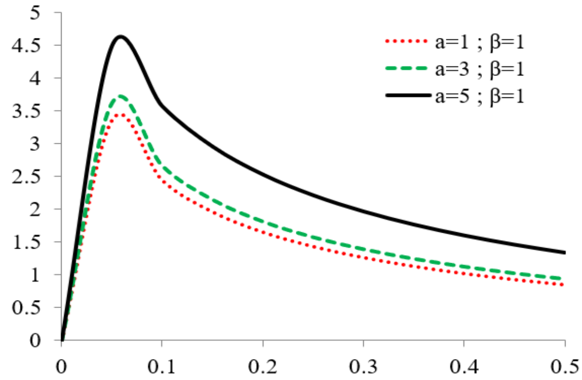


**Figure 4.** Axial concentration profile.

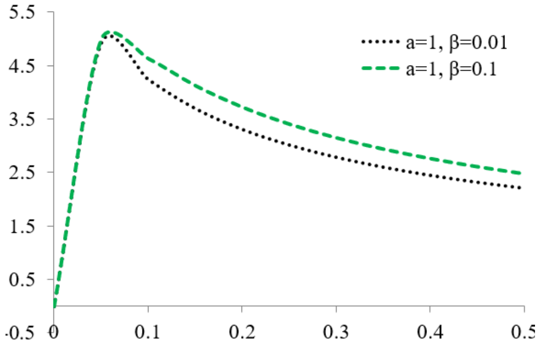


**Figure 5.** Axial concentration profile.

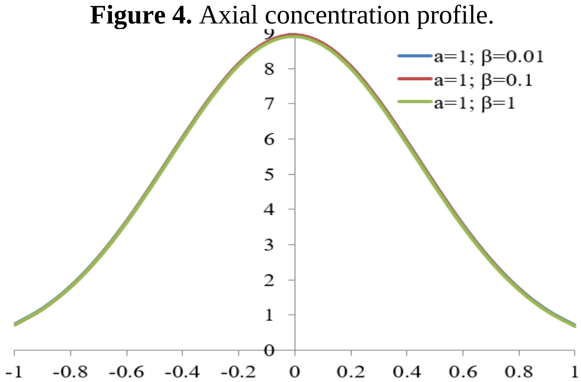


**Figure 6.** Axial concentration profile versus $X$.

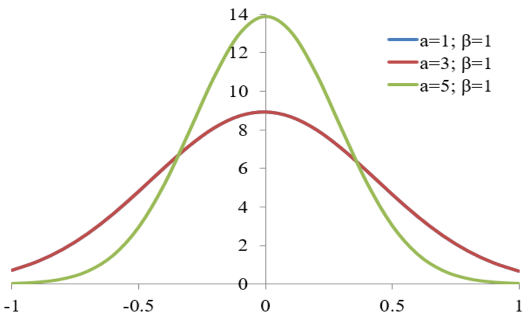


**Figure 7.** Axial concentration profile versus $X$.

The velocity profile is represented in Figure 3 for different values of the couple stress parameter ‘a’. As ‘a’ increases, velocity decreases due to an increase in the spinning of suspended particles. Figures 3 and 4 show a plot of the exchange coefficient. $-M_0$ versus t. $M_0$ is constant for small times, increases for moderate time levels, and reaches a constant value at large times. As the reaction (absorption) parameter at the wall increases $-M_0$ has a higher value at small- and moderate-time levels. But at a large time level, it reaches a constant value for all values of β. It is not affected by a couple of stress parameters as it is independent of velocity.

Figures 5 and 6 show the concentration profile versus time for different values of the couple stress parameter and reaction coefficient at X = 0.5. Figure 5 shows that concentration increases with a couple of stress parameters ‘a’. This is because velocity is inversely proportional to ‘a’, and more solute gets convicted as the couple stress parameter decreases. For small time, concentration is not affected by the reaction coefficient but increases with β in large time levels.

Figure 7 shows the axial concentration profile for different time levels. At t = 0, the whole curve is situated between x = -1 and x = 1, with a maximum of x = 0. As t increases, it spreads from x = -2 to x = 2 for t = 0.05 and x = -3 to x = 3 for t = 0.1. This figure shows the actual dispersion along the axial direction as time progresses.

## 5. Conclusions

This problem analyzes convective diffusive mass transfer in the presence of suction and injection. The change in velocity profile affects the concentration due to the presence of suction and injection. Velocity profile shows deviation from original parabolic profile. This analysis can be used to study any situation where solute transfer of injected solute is considered in the presence of suction and injection.

## Funding

This research received no external funding.

## Acknowledgments

The authors declare no acknowledgment.

## Conflicts of Interest

The authors declare no conflict of interest.

## References

1. Srivastava, L.M. Flow of couple stress fluid through stenotic blood vessels. *J. Biomech*. **1985**, *18*, 479–485, https://doi.org/10.1016/0021-9290(85)90662-1.
2. Devakar, M.; Iyengar, T.K.V.K.V. Stokes' Problems for an Incompressible Couple Stress Fluid. *Nonlinear Anal.: Model. Control.* **2008**, *13*, 181-190, https://doi.org/10.15388/na.2008.13.2.14578.
3. Devakar, M.; Sreenivasu, D.; Shankar, B. Analytical solutions of couple stress fluid flows with slip boundary conditions. *Alex. Eng. J.* **2014**, *53*, 723-730, https://doi.org/10.1016/j.aej.2014.06.005.
4. Ramzan, M.; Farooq, M.; Alsaedi, A.; Hayat, T. MHD three-dimensional flow of couple stress fluid with Newtonian heating. *Eur. Phys. J. Plus.* **2013**, *128*, 49, https://doi.org/10.1140/epjp/i2013-13049-5.
5. Kumar, T.S. Hybrid nanofluid slip flow and heat transfer over a stretching surface. *Partial Differ. Equ. Appl. Math*. **2021**, *4*, 100070, https://doi.org/10.1016/j.padiff.2021.100070.
6. Xiong, P.-Y.; Nazeer, M.; Hussain, F.; Ijaz Khan, M.; Saleem, A.; Qayyum, S.; Chu, Y.-M. Two-phase flow of couple stress fluid thermally effected slip boundary conditions: Numerical analysis with variable liquids properties. *Alex. Eng. J*. **2022**, *61*, 3821–3830, https://doi.org/10.1016/j.aej.2021.09.012.

7. Shilpa, B.; Leela, V.; Prasannakumara, B.C.; Nagabhushana, P. Soret and Dufour effects on MHD double-diffusive mixed convective heat and mass transfer of couple stress fluid in a channel formed by electrically conducting and non-conducting walls. *Waves Random Complex Media* **2022**, 1-22, https://doi.org/10.1080/17455030.2022.2119491.
8. Gaikwad, S.N.; Rangdal, P.B. Effect of Gravity and Throughflow on Double Diffusive Convection in a Couple Stress Fluid Saturated Porous Media. *J. Adv. Res. Fluid Mech. Therm. Sci.* **2023**, *101*, 121–136, https://doi.org/10.37934/arfmts.101.1.121136.
9. Prasad, K.V.; Choudhari, R.; Vaidya, H.; Bhat, A.; Animasaun, I.L. Analysis of couple stress nanofluid flow under convective condition in the temperature-dependent fluid properties and Lorentz forces. *Heat Transf.* **2023**, *52*, 216–235, https://doi.org/10.1002/htj.22692.
10. Mkhatshwa, M.P.; Motsa, S.S.; Sibanda, P. MHD Mixed Convection Flow of Couple Stress Fluid Over an Oscillatory Stretching Sheet with Thermophoresis and Thermal Diffusion Using the Overlapping Multi-domain Spectral Relaxation Approach. *Int. J. Appl. Comput. Math.* **2021**, *7*, 93, https://doi.org/10.1007/s40819-021-01043-0.
11. Raghunatha, K.R.; Shivakumara, I.S.; Pallavi, G. Couple stress effects on the stability of three-component convection-diffusion in a porous layer. *Heat Transf.* **2021**, *50*, 3047-3064, https://doi.org/10.1002/htj.22017.
12. Bilal, M.; Saeed, A.; Gul, T.; Rehman, M.; Khan, A. Thin-film flow of Carreau fluid over a stretching surface including the couple stress and uniform magnetic field. *Partial Differ. Equ. Appl. Maths.* **2021**, *4*, 100162, https://doi.org/10.1016/j.padiff.2021.100162.
13. Ramesh, K.; Reddy, M.G.; Souayeh, B. Electro-magneto-hydrodynamic flow of couple stress nanofluids in micro-peristaltic channel with slip and convective conditions. *Appl. Math. Mech.* **2021**, *42*, 593–606, https://doi.org/10.1007/s10483-021-2727-8.
14. Sankarasubramanian, R.; Gill, W.N. Unsteady convective diffusion with interphase mass transfer. *Proc. R. Soc. A: Math. Phys. Eng. Sci.* **1973**, *333*, 115–132, https://doi.org/10.1098/rspa.1973.0051.
15. Roy, A.K.; Bég, O.A. Mathematical modeling of unsteady solute dispersion in two-fluid (micropolar-Newtonian) blood flow with bulk reaction. *Int. Commun. Heat Mass Transf.* **2021**, *122*, 105169, https://doi.org/10.1016/j.icheatmasstransfer.2021.105169.
16. Zhang, Y.; Ding, B.; Zhao, D.-Y.; Zhao, S.; Gong, L. Effect of natural convection and diffusion on liquid-liquid phase separation behaviors of partially miscible solutions with lower critical solution temperature. *Int. J. Heat Mass Transf.* **2023**, *201*, 123566, https://doi.org/10.1016/j.ijheatmasstransfer.2022.123566.
17. Nandeppanavar, M.M.; Kemparaju, M.C.; Raveendra, N. Effect of Richardson number on double-diffusive mixed convective slip flow, Heat and Mass transfer of MHD Casson fluid. *Proc. Inst. Mech. Eng. E: J. Process Mech. Eng.* **2022**, *236*, 1958–1966, https://doi.org/10.1177/09544089221079264.
18. Roy, A.K.; Bég, O.A. Asymptotic study of unsteady mass transfer through a rigid artery with multiple irregular stenoses. *Appl. Math. Comput.* **2021**, *410*, 126485, https://doi.org/10.1016/j.amc.2021.126485.
19. Sushma, T.C.; Nalinakshi, N.; Dinesh, P.A.; Jayalakshmamma, D.V.; Kumar, T.S. Convective heat transfer and MHD flow through semi-porous cylindrical filters embedded in an impermeable region. *Chin. J. Phys.* **2023**, *81*, 9–25, https://doi.org/10.1016/j.cjph.2022.10.015.
20. Weijermars, R. Diffusive Mass Transfer and Gaussian Pressure Transient Solutions for Porous Media. *Fluids* **2021**, *6*, 379, https://doi.org/10.3390/fluids6110379.
21. Abbas, A.; Shafqat, R.; Jeelani, M.B.; Alharthi, N.H. Convective Heat and Mass Transfer in Third-Grade Fluid with Darcy–Forchheimer Relation in the Presence of Thermal-Diffusion and Diffusion-Thermo Effects over an Exponentially Inclined Stretching Sheet Surrounded by a Porous Medium: A CFD Study. *Processes* **2022**, *10*, 776, https://doi.org/10.3390/pr10040776.
22. Zhao, B.-X.; Yang, J.-Q.; Numerical investigation of 2D double-diffusive convection in rectangular cavities with different aspect ratios: Heat and mass transfer and flow characteristics. *Phys. Fluids* **2022**, *34*, 034120, https://doi.org/10.1063/5.0084537.
23. Obulesu, M.; Raghunath, K.; Charankumar, G.; Ramu, S.; Giulio, L. MHD Heat and Mass Transfer Steady Flow of a Convective Fluid Through a Porous Plate in The Presence of Diffusion Thermo and Aligned Magnetic Field. *J. Adv. Res. Fluid Mech.* **2022**, *89*, 62–76, https://doi.org/10.37934/arfmts.89.1.6276.
24. Uddin, M.J.; Rasel, S.K.; Adewole, J.K.; Al Kalbani, K.S. Finite element simulation on the convective double diffusive water-based copper oxide nanofluid flow in a square cavity having vertical wavy surfaces in presence of hydro-magnetic field. *Results Eng.* **2022**, *13*, 100364, https://doi.org/10.1016/j.rineng.2022.100364.

25. Zari, I.; Shafiq, A.; Khan, T.S. Simulation study of Marangoni convective flow of kerosene oil based nanofluid driven by a porous surface with suction and injection. *Int. Commun. Heat Mass Transf*. **2021**, *127*, 105493, https://doi.org/10.1016/j.icheatmasstransfer.2021.105493.
26. Ali, B.; Shafiq, A.; Siddique, I.; Al-Mdallal, Q.; Jarad, F. Significance of suction/injection, gravity modulation, thermal radiation, and magnetohydrodynamic on dynamics of micropolar fluid subject to an inclined sheet via finite element approach. *Case Stud. Therm. Eng.* **2021**, *28*, 101537, https://doi.org/10.1016/j.csite.2021.101537.
27. Kumar, M.A.; Reddy, Y.D.; Goud, B.S.; Rao, V.S. Effects of soret, dufour, hall current and rotation on MHD natural convective heat and mass transfer flow past an accelerated vertical plate through a porous medium. *Int. J. Thermofluids* **2021**, *9*, 100061, https://doi.org/10.1016/j.ijft.2020.100061.